



# Synthesis, structure and bonding of a digold complex with bridging triphenylstannyl ligands



Richard D. Adams\*, Yuen Onn Wong, Qiang Zhang

Department of Chemistry and Biochemistry, University of South Carolina, Columbia, SC 29208, USA

## ARTICLE INFO

### Article history:

Received 30 November 2014

Received in revised form

15 January 2015

Accepted 25 January 2015

Available online 13 February 2015

Dedicated to Professor Hubert Schmidbaur  
on the occasion of his 80th birthday.

### Keywords:

Gold

Tin

Molecular orbitals

Crystal structure

## ABSTRACT

The reaction of  $\text{Au}(\text{PPh}_3)\text{Ph}$  with  $\text{HSnPh}_3$  yielded the new digold–ditin complex,  $[\text{Au}(\text{PPh}_3)(\mu-\text{SnPh}_3)]_2$ , **6** in 52% yield. Benzene was also formed.  $\text{Sn}_2\text{Ph}_6$  is a major coproduct that was formed by the degradation of **6**. Compound **6** was characterized structurally by a single-crystal X-ray diffraction analysis. The molecule contains two  $\text{Au}(\text{PPh}_3)$  groups that are joined by a strong Au–Au bond (2.5590(5) Å in length) that is bridged by two  $\text{SnPh}_3$  groups. The metal–metal bonding was analyzed by DFT Mo calculations. The Au–Sn bonding is represented by the HOMO which is a four center: two electron bond.

© 2015 Elsevier B.V. All rights reserved.

## Introduction

Interest in the organometallic chemistry of gold has grown rapidly in recent years following the discoveries that gold nanoparticles supported on metal oxides exhibit surprisingly high activity for the catalytic oxidation of CO and selected hydrocarbons [1]. Studies have also shown bimetallic catalysts containing gold exhibit even better activity for oxidation catalysis [2]. Tin is well known for its ability to serve as a modifier of heterogeneous metal catalysts [3]. A recent study has shown that  $\text{Au/SnO}_2$  catalyst exhibits oxidation activity comparable to  $\text{Au/TiO}_2$ , one of the most active catalytic gold oxidation systems [4]. Gold complexes can also perform novel forms of dual catalysis homogeneously when combined with other metals, most notably with palladium [5].

There are very few examples of organometallic gold–tin complexes in the literature. Examples with terminally-coordinated tin ligands include  $\text{Au}(\text{PMe}_2\text{Ph})_2(\text{SnCl}_3)$ , **1**,  $\text{Au–Sn} = 2.881(1)$  Å [6] and  $\text{Au}(\text{PPh}_3)[\text{Sn}\{\text{N}(p\text{-tol})\text{SiMe}_2\}_3\text{SiMe}]$ , **2** [7], see Scheme 1.

Compounds  $[\text{Au}_4(\text{PPh}_3)_4(\mu-\text{SnCl}_3)_2]$ , **3** [8] and  $\text{Au}_4(\text{PPh}_3)_4[\mu-\text{SnCB}_{10}\text{H}_{11}]_2$ , **4** [9] and the dianion compound  $[\text{Bu}_3\text{NH}]_2[(\text{PPh}_3)\text{Au}(\mu-\text{SnB}_{11}\text{H}_{11})_2]$ , **5** [10] have bridging Sn ligands, Scheme 2.

We have recently found that aryl containing gold phosphine complexes,  $\text{Au}(\text{PPh}_3)\text{Ar}$ , Ar = Ph, Np, Py, react with certain dirhenium [11] and triosmium [12] carbonyl complexes to yield electronically unsaturated complexes containing bridging aryl ligands. In the present work, we have investigated the reaction of  $\text{Au}(\text{PPh}_3)\text{Ph}$  with  $\text{HSnPh}_3$ . The principal product is a new digold–ditin complex  $[\text{Au}(\text{PPh}_3)(\mu-\text{SnPh}_3)]_2$ , **6** that contains two bridging  $\text{SnPh}_3$  ligands. The results of our studies of the synthesis, structural characterization and bonding in this compound are described in this report.

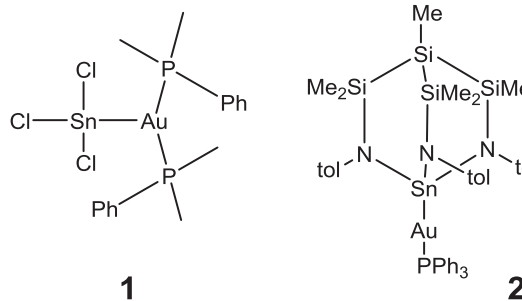
## Experimental details

### General data

Reagent grade solvents were dried by the standard procedures and were freshly distilled prior to use. Infrared spectra were recorded on a Thermo Nicolet Avatar 360 FT-IR spectrophotometer.  $^1\text{H}$  NMR and  $^{31}\text{P}\{^1\text{H}\}$  NMR were recorded on a Varian Mercury 400 spectrometer operating at 400.1 and 161.9 MHz respectively.  $^{31}\text{P}\{^1\text{H}\}$  NMR spectra were referenced externally by using 85% *ortho*- $\text{H}_3\text{PO}_4$ . Solid state  $^{119}\text{Sn}$  cross-polarization magic angle spinning (CP-MAS) spectra were collected on a Bruker Avance III-HD 500 MHz spectrometer fitted with a 1.9 mm MAS probe and were

\* Corresponding author.

E-mail address: [Adamsrd@mailbox.sc.edu](mailto:Adamsrd@mailbox.sc.edu) (R.D. Adams).

**Scheme 1.** Line structures for compounds **1** and **2**.

referenced against  $\text{SnPh}_4$ . The spectra was collected at ambient temperature with a sample rotation rate of 20 kHz.  $\text{HSnPh}_3$  was obtained from SIGMA-ALDRICH and was used without further purification.  $\text{Au}(\text{PPh}_3)\text{Ph}$  was prepared according to the previously reported procedure [13]. Product separations were performed by TLC in air on Analtech 0.25 mm alumina 60 Å  $F_{254}$  glass plates.

### Reaction of $\text{HSnPh}_3$ with $\text{Au}(\text{PPh}_3)\text{Ph}$

30.0 mg (0.026 mmol) of  $\text{Au}(\text{PPh}_3)\text{Ph}$  was added to 18.6 mg (0.052 mmol) of  $\text{HSnPh}_3$  dissolved in 10 mL of benzene. The solution was allowed to stir for 7 h at room temperature. A red-orange solution formed and the solvent was then removed *in vacuo*. The residue was extracted in methylene chloride and separated by TLC by using hexane solvent to elute a yellow band of  $[\text{Au}(\text{PPh}_3)(\mu\text{-SnPh}_3)]_2$ , **6** 18.8 mg (52%) and  $\text{Sn}_2\text{Ph}_6$ , 8.6 mg (46%). The orange crystals of pure **6** can be physically separated from the colorless crystals of the  $\text{Sn}_2\text{Ph}_6$ . Spectral data for **6**:  $^1\text{H}$  NMR ( $\text{CD}_2\text{Cl}_2$ , in ppm)  $\delta$  = 7.50 (m, 15H), 7.35 (m, 15H).  $^{119}\text{Sn}$  CP-MAS (in ppm)  $\delta$  = 121.01 (s).  $^{31}\text{P}$  NMR ( $\text{CD}_2\text{Cl}_2$ , in ppm)  $\delta$  = 43.33 (s). Anal. Calcd for **1**: C, 53.42; H, 3.73. Found: C, 56.65; H, 4.10. Samples of **6** inevitably contain small amounts of  $\text{Sn}_2(\text{C}_6\text{H}_5)_6$  formed by its decomposition. This could explain the high measurements for C and H.

### Crystallographic analysis

Orange single crystals of **6** crystallize together with colorless crystals of  $\text{Sn}_2\text{Ph}_6$  (a decomposition product) upon slow evaporation of solvent from a solution in methylene chloride at 15 °C. An orange crystal of **6** was glued onto the end of a thin glass fiber. X-ray intensity data were measured by using a Bruker SMART APEX CCD-based diffractometer by using Mo K $\alpha$  radiation ( $\lambda = 0.71073 \text{ \AA}$ ). The raw data frames were integrated with the SAINT + program by using a narrow-frame integration algorithm [14]. Correction for Lorentz and polarization effects were also applied by using SAINT+. An empirical absorption correction based on the multiple measurement of equivalent reflections was applied by using the

**Table 1**  
Crystallographic data for **6**.

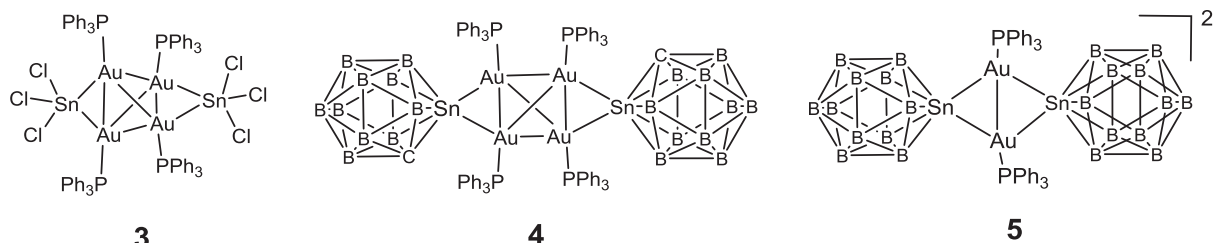
Empirical formula	$\text{Au}_2\text{Sn}_2\text{P}_2\text{C}_{72}\text{H}_{60} \cdot \text{CH}_2\text{Cl}_2$
Formula weight	1618.54
Crystal system	Orthorhombic
<i>Lattice parameters</i>	
<i>a</i> (Å)	14.2638(6)
<i>b</i> (Å)	22.9477(9)
<i>c</i> (Å)	9.8436(4)
$\alpha$ (deg)	90.00
$\beta$ (deg)	90.00
$\gamma$ (deg)	90.00
<i>V</i> (Å $^3$ )	3222.0(2)
Space group	$P_{2}1_2_1_2$
<i>Z</i> value	2
$\rho_{\text{calc}}$ (g/cm $^3$ )	1.71
$\mu$ (Mo K $\alpha$ ) (mm $^{-1}$ )	5.437
Temperature (K)	294(2)
$2\theta_{\text{max}}(^{\circ})$	47.50
No. obs. ( $I > 2\sigma(I)$ )	7132
No. parameters	364
Goodness of fit (GOF) <sup>a</sup>	1.119
Max. shift on final cycle of refinement	0.001
Residuals <sup>a</sup> : $R$ ; $R_w$	0.0424; 0.1092
Absorption correction, max/min	Multi-Scan 1.000/0.699
Largest peak in Final Diff. Map (e $^-/\text{\AA}^3$ )	2.019

<sup>a</sup>  $R = \sum_{hkl} (|F_{\text{obs}}| - |F_{\text{calcd}}|)/\sum_{hkl} |F_{\text{obs}}|$ ;  $R_w = [\sum_{hkl} w(|F_{\text{obs}}| - |F_{\text{calcd}}|)^2/\sum_{hkl} w F_{\text{obs}}^2]^{1/2}$ ;  $w = 1/\sigma^2(F_{\text{obs}})$ ; GOF =  $[\sum_{hkl} w(|F_{\text{obs}}| - |F_{\text{calcd}}|)^2/(n_{\text{data}} - n_{\text{vari}})]^{1/2}$ .

program SADABS. The structure was solved by a combination of direct methods and difference Fourier syntheses, and refined by full-matrix least-squares on  $F^2$ , using the SHELXTL software package [15]. All non-hydrogen atoms were refined with anisotropic displacement parameters. The hydrogen atoms were placed in geometrically idealized positions and included as standard riding atoms during the final cycles of least-squares refinements. Compound **6** crystallized in the orthorhombic crystal system with one equivalent of  $\text{CH}_2\text{Cl}_2$  cocrystallized from the crystallization solvent. The space group  $P_{2}1_2_1_2$  was uniquely identified by the pattern of systematic absences observed in the data. Crystal data, data collection parameters, and results of the analyses are listed in Table 1.

### Computational details

Density functional theory (DFT) calculations were performed with the Amsterdam Density Functional (ADF) suite of programs [16] by using the PBEsol functional [17] with valence quadruple- $\zeta + 4$  polarization function, relativistically-optimized (QZ4P) basis sets for the gold, tin, phosphorus, carbon and hydrogen atoms with frozen cores. The molecular orbitals for compound **6** and their energies were determined by geometry-optimized calculations with scalar relativistic corrections that were initiated by using the atom positional parameters for the molecule as determined from

**Scheme 2.** Structures of **3**, **4** and the anion of **5**.

the crystal structure analysis. The geometry-optimized coordinates of **6** are given in Table S1.

## Results and discussion

The reaction of  $\text{Au}(\text{PPh}_3)\text{Ph}$  with  $\text{HSnPh}_3$  yielded the new digold–ditin complex,  $[\text{Au}(\text{PPh}_3)(\mu\text{-SnPh}_3)]_2$ , **6** in 52% yield.  $\text{Sn}_2\text{Ph}_6$  was a major coproduct that was obtained in 46% yield.  $\text{Sn}_2\text{Ph}_6$  was subsequently found to be formed by the degradation of **6**. The formation of benzene was observed when the reaction was performed in an NMR tube in  $\text{CD}_2\text{Cl}_2$  solvent. Compound **6** was characterized structurally by a single-crystal X-ray diffraction analysis. An ORTEP diagram of its molecular structure is shown in Fig. 1. The molecule contains two  $\text{Au}(\text{PPh}_3)$  groups that are joined by a strong Au–Au bond that is bridged by two  $\text{SnPh}_3$  groups. In the solid state the molecule lies on a crystallographic two-fold rotation axis that lies perpendicular to the Au–Au bond. The Au–Au distance in **6** is short, 2.5590(5) Å, and is shorter than the Au–Au bond distance found in the  $\text{SnB}_{11}\text{H}_{11}$ -bridged digold dianion of compound **5**,  $\text{Au}–\text{Au} = 2.625(1)$  Å (Scheme 2) [10]. The  $\text{P}–\text{Au}–\text{Au}^{\dagger}$  angle in **6**, 170.74(5)°, is almost linear and is similar to that in **5**, 178.78(4)°. Mingos described the structure of digold molecule  $\text{Ph}_3\text{AuAuPPPh}_3$  **7** which has no bridging ligands [18]; the Au–Au distance given for **7** is 2.76 Å. Although the identity of **7** has recently been questioned [19], Bertrand recently reported a related unbridged digold–dicarbene complex ( $\text{CAAC}$ ) $\text{AuAu}(\text{CAAC})$ , **8** ( $\text{CAAC} = \text{cyclic(alkyl)(amino)carbene}$ ) [20] that contains a very short Au–Au bond, 2.5520(6) Å having nearly linear C–Au–Au angles, 173.8(2)° and 171.3(3)°. The shortest reported Au–Au bond distances are for the complexes  $[\text{Au}_2(\text{hpp})_2\text{Cl}_2]$ ,  $\text{Au}–\text{Au} = 2.4752(9)$  Å,  $[(\text{PhCO}_2)_6\text{Au}_4(\text{hpp})_2\text{Ag}_2]$ ,  $\text{Au}–\text{Au} = 2.4473(19)$  Å,  $\text{hpp} = 3,4,6,7,8,9$ -hexahydro-pyrimido[1,2-a]pyrimidinate [21]. Compound **6** contains two independent Au–Sn distances,  $\text{Au}1–\text{Sn}1 = 2.8207(16)$  Å and  $\text{Au}1–\text{Sn}1^{\dagger} = 2.9038(6)$  Å that are statistically different in length. This is probably due to the rotational conformation of the  $\text{SnPh}_3$  group. These distances are much longer than that to

the terminally coordinated tin ligand in compound **2**,  $\text{Au}–\text{Sn} = 2.5651(13)$  Å [7], but are similar to the bridging Au–Sn distances reported for the compounds **3**, 2.8150(7) Å and 2.9725(8) Å [8]; **4**, 2.891(1) Å, 2.727(1) Å, 2.936(1) Å, and 2.757(1) [9] and the dianion **5**, 2.737(1) Å and 2.761(1) Å [10] (see Scheme 2). The  $\text{Au}–\text{Sn}–\text{Au}$  angle in **6** (53.08°) is slightly smaller than the  $\text{Au}–\text{Sn}–\text{Au}$  angle (57.03°) in **5** as a result of the shorter  $\text{Au}–\text{Au}$  distance in **6**. The  $\text{Au}_2\text{Sn}_2$  ring is almost planar; the dihedral angle between the two  $\text{Au}_2\text{Sn}$  triangles is 163.57(2)°. It is unlikely that there is any significant direct Sn–Sn bonding interaction, because the  $\text{Sn} \cdots \text{Sn}$  distance is very long at 5.069(1) Å. Compound **6** does not exhibit a  $^{119}\text{Sn}$  NMR signal in solutions; however, a  $^{119}\text{Sn}$  CP-MAS spectrum of **6** does show a singlet at  $\delta = 121.01$  in the solid state. This is consistent with the solid state structure having equivalent tin atoms. The  $^{119}\text{Sn}$  CP-MAS spectrum of  $\text{Sn}_2\text{Ph}_6$  in the solid state shows a singlet at  $\delta = -142.1$ .

There are very few examples of complexes containing bridging  $\text{SnPh}_3$  ligands. Bridging  $\text{SnPh}_3$  groups were found across the unsaturated M–M bond of the dinuclear transition metal complexes  $[\text{M}_2\text{Cp}_2(\mu\text{-SnPh}_3)(\mu\text{-PCy}_2)(\text{CO})_2]$ ,  $\text{M} = \text{Mo}$  [22],  $\text{M} = \text{W}$  [23]; across a Ge–Ge edge of the complex polyhedral anion  $[\text{Ge}_9(\mu\text{-SnPh}_3)]^{3-}$  [24]; and across a B–B edge of the polyhedral borane  $\text{B}_5\text{H}_8(2,3\text{-}\mu\text{-SnPh}_3)$  [25]. It is unusual to have a  $\text{SnPh}_3$  group bridging two metal atoms because the tin atom has only one unpaired valence electron. Clearly some sort of multicenter delocalized bonding can be anticipated for the Au–Sn bonding in the cluster of **6**.

In order to understand the Au–Au and Au–Sn bonding in **6**, geometry-optimized DFT molecular orbital calculations were performed. Selected molecular orbitals (MOs) that show the metal–metal orbital interactions in the  $\text{Au}_2\text{Sn}_2$  ring are shown in Fig. 2. The LUMO (-2.21 eV) is a  $\pi$ -type MO delocalized across all four atoms. The HOMO (-4.30 eV) is a delocalized four center – two electron  $\sigma$ -type orbital that shows the nature of the gold–tin bonding interactions, but it has a node along the Au–Au vector. Because of this node, this orbital makes no significant contribution to direct bonding between the two gold atoms. The HOMO-1 (-5.69 eV) is a symmetric two electron bond that is composed principally of d-orbitals from the Au atoms and with small contributions from atomic p-orbitals on the two Sn atoms. This orbital confirms the existence of a significant direct Au–Au  $\sigma$ -bonding interaction. By using conventional electron counting procedures, the Au–Sn bonding in **6** would be best described schematically by the diagram A where the four dashed lines represent the four pairs of Au–Sn interactions represented by the HOMO, formally 1/4 of a bond for each Au–Sn interaction, and the solid line between the two Au atoms is formally an Au–Au single bond that is represented by the HOMO-1.

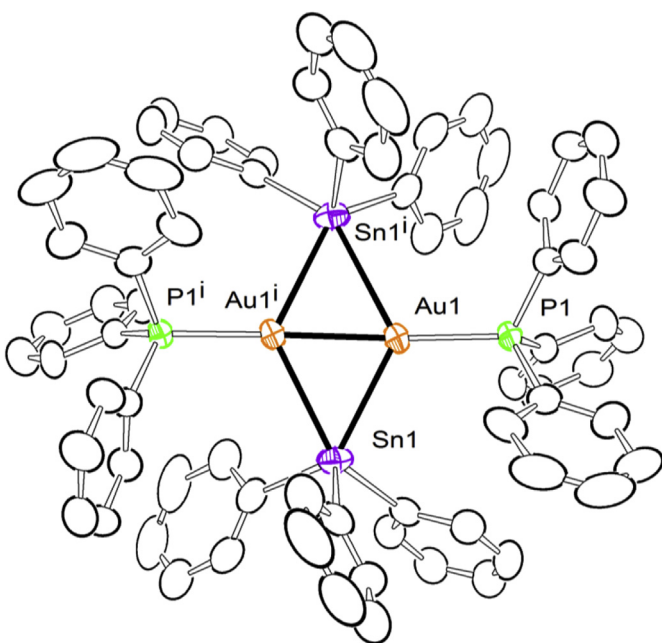
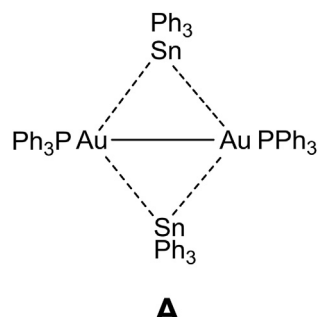


**Fig. 1.** An ORTEP diagram of the molecular structure of  $[(\text{AuPPh}_3)(\mu\text{-SnPh}_3)]_2$ , **6**, showing 30% thermal ellipsoid probability.



The complete DFT analysis also reveals three low-lying orbitals that show favorable overlaps that could be interpreted as

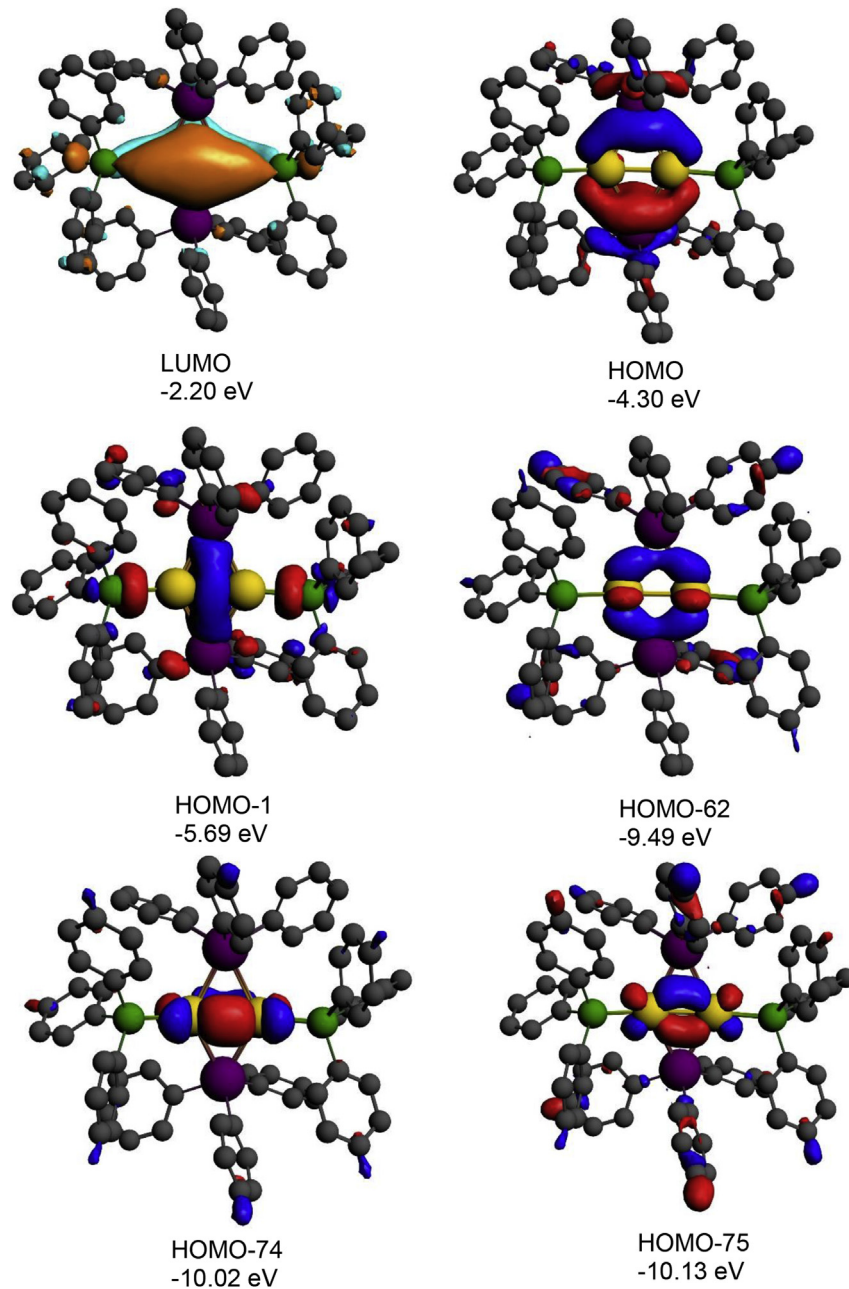


**Fig. 2.** Selected molecular orbitals with calculated energies in electron volts (eV) for the LUMO, HOMO, HOMO-1, HOMO-62, HOMO-74 and HOMO-75 of **6**.

supplementary metal–metal bonding. These are the HOMO-62, the HOMO-74 and HOMO-75. The HOMO-62 shows gold–tin bonding interactions and the HOMO-74 and HOMO-75 both show  $\pi$ -overlaps derived from Au d-orbitals, see Fig. 2, but because of their low

energies they probably do not make major contributions to the total of the metal–metal bonding (Tables 2 and 3).

Curiously, a number of years ago Schmidbaur reported the compound  $\text{Au}(\text{PPh}_3)(\text{GeCl}_3)$ , **9** which was shown to be a dimer in the solid state and contained a significant, but long Au–Au

**Table 2**

Selected intramolecular distances and angles for **6** from the X-ray structural analysis.<sup>a</sup>

Atom	Atom	Distance (Å)	Atom	Atom	Atom	Angle (°)
Au1	Sn1	2.8207(6)	Au1	Sn1	Au1 <sup>i</sup>	53.083(13)
Au1	Sn1 <sup>i</sup>	2.9038(6)	Sn1	Au1	Sn1 <sup>i</sup>	124.613(15)
Au1	Au1 <sup>i</sup>	2.5590(5)	P1	Au1	Au1 <sup>i</sup>	170.74(5)
Au1	P1	2.3336(17)				
Sn1	Sn1 <sup>i</sup>	5.069(1)				

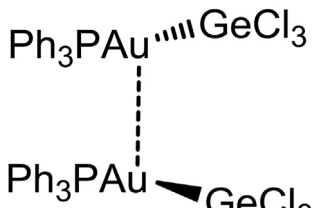
<sup>a</sup> Estimated standard deviations in the least significant figure are given in parentheses. *i* = symmetry related position.

**Table 3**

Interatomic distances for the DFT geometry-optimized structure of **6**.

Atom	Atom	Distance (Å)	Atom	Atom	Atom	Angle (°)
Au1	Sn1	2.806	Au1	Sn1	Au1 <sup>i</sup>	53.7
Au1	Sn1 <sup>i</sup>	2.835	Sn1	Au1	Sn1 <sup>i</sup>	124.1
Au1	Au1 <sup>i</sup>	2.552				
Au1	P	2.375				

aurophilic interaction, 2.960(1) Å, but the GeCl<sub>3</sub> ligands are not of a bridging type [26].



9

## Conclusions

Compound **6** is a dimer of the formula unit “Au(PPh<sub>3</sub>)(SnPh<sub>3</sub>)”. The molecule is held together by a strong direct Au–Au σ-bonding interaction and two bridging SnPh<sub>3</sub> ligands. The Au–Sn bonding is best described by a four center – two electron bond having a node along the Au–Au vector.

## Acknowledgments

This research was supported by the following grants from the National Science Foundation: CHE-1111496 and CHE-1048629. Many thanks to Professor John Fackler for helpful discussions.

## Appendix A. Supplementary data

CCDC 1035628 for compound **6** contains the supplementary crystallographic data for this paper. These data can be obtained free of charge from The Cambridge Crystallographic Data Centre via [www.ccdc.cam.ac.uk/data\\_request/cif](http://www.ccdc.cam.ac.uk/data_request/cif).

## Appendix B. Supplementary data

Supplementary data related to this article can be found at <http://dx.doi.org/10.1016/j.jorganchem.2015.01.021>.

## References

- [1] (a) G. Li, R. Jin, *Acc. Chem. Res.* 46 (2013) 1749–1758;  
 (b) M. Haruta, *Gold Bull.* 37 (2004) 27–36;  
 (c) M. Haruta, *Catal. Today* 36 (1997) 153–166;  
 (d) M. Haruta, M. Date, *Appl. Catal. A: Gen.* 222 (2001) 427–437;  
 (e) J. Oliver-Meseguer, J.R. Cabrero-Antonino, I. Dominguez, A. Leyva-Perea, A. Corma, *Science* 338 (2012) 1452–1455;  
 (f) A.S.K. Hashmi, G.J. Hutchings, *Angew. Chem. Int. Ed.* 45 (2006) 7896–7936;  
 (g) C. Della Pina, E. Falletta, L. Prati, M. Rossi, *Chem. Soc. Rev.* 37 (2008) 2077–2095;  
 (h) S. Lee, L.M. Molina, M.J. Lopez, J.A. Alonso, B. Hammer, B. Lee, S. Seifert, R.E. Winans, J.W. Elam, M.J. Pellin, S. Vajda, *Angew. Chem. Int. Ed.* 48 (2009) 1467–1471;  
 (i) A.A. Herzing, C.J. Kiely, A.F. Carley, P. Landon, G.J. Hutchings, *Science* 32 (2008) 1331–1335;  
 (j) L. Zhang, *Acc. Chem. Res.* 47 (2014) 877–888.
- [2] (a) S.J. Freakley, Q. He, C.J. Kiely, G.J. Hutchings, *Catal. Lett.* 145 (2015) 71–79;  
 (b) G.J. Hutchings, C.J. Kiely, *Acc. Chem. Res.* 46 (2013) 1759–1772;
- (c) G.J. Hutchings, *Catal. Today* 238 (2014) 69–73;  
 (d) Y. Zhang, X. Cui, F. Shi, Y. Deng, *Chem. Rev.* 112 (2012) 2467–2505;  
 (e) G.J. Hutchings, *Chem. Commun.* (2008) 1148–1164;  
 (f) J.A. Lopez-Sanchez, N. Dimitratos, N. Glanville, L. Kesavan, C. Hammond, J.K. Edwards, A.F. Carley, C. Kiely, G.J. Hutchings, *Appl. Catal. A: Gen.* 391 (2011) 400–406;  
 (g) D.I. Enache, J.K. Edwards, P. Landon, B. Solsona-Espriu, A.F. Carley, A.A. Herzing, M. Watanabe, C.J. Kiely, D.W. Knight, G.J. Hutchings, *Science* 311 (2006) 362–365;  
 (h) P. Miedziak, M. Sankar, M. Dimitratos, J.A. Lopez-Sanchez, A.F. Carley, D.W. Knight, S.H. Taylor, C.J. Kiely, G.J. Hutchings, *Catal. Today* 164 (2011) 315–319;  
 (i) R. Wang, Z. Zhiwei Wu, C. Chen, Z. Zhangfeng Qin, H. Zhu, G. Wang, H. Wang, C. Wu, W. Dong, W. Fan, J. Wang, *Chem. Commun.* 49 (2013) 8250–8252;  
 (j) L. Kesavan, R. Tiruvalam, M.H. Ab Rahim, M.I. bin Saiman, D.I. Enache, R.L. Jenkins, N. Dimitratos, J.A. Lopez-Sanchez, S.H. Taylor, D.W. Knight, C.J. Kiely, G.J. Hutchings, *Science* 331 (2011) 195–199.
- [3] (a) J.M. Thomas, B.F.G. Johnson, R. Raja, G. Sankar, P.A. Midgley, *Acc. Chem. Res.* 36 (2003) 20;  
 (b) A.B. Hungria, R. Raja, R.D. Adams, B. Captain, J.M. Thomas, P.A. Midgley, V. Golvenko, B.F.G. Johnson, *Angew. Chem. Int. Ed.* 45 (2006) 4782–4785;  
 (c) R.D. Adams, E.M. Boswell, B. Captain, A.B. Hungria, P.A. Midgley, R. Raja, J.M. Thomas, *Angew. Chem. Int. Ed.* 46 (2007) 8182–8185;  
 (d) R.D. Adams, D.A. Blom, B. Captain, R. Raja, J.M. Thomas, E. Trufan, *Langmuir* 24 (2008) 9223–9226;  
 (e) R.D. Adams, E. Trufan, *Phil. Trans. R. Soc.* 368 (2010) 1473–1493;  
 (f) R. Burch, *J. Catal.* 71 (1981) 348–359;  
 (g) R. Burch, L.C. Garla, *J. Catal.* 71 (1981) 360–372.
- [4] Y. Maeda, T. Akita, M. Kohyama, *Catal. Lett.* 144 (2014) 2086–2090.
- [5] (a) J.J. Hirner, Y. Shi, S.A. Blum, *Accts. Chem. Res.* 44 (2011) 603–613;  
 (b) M. Al-Amin, K.E. Roth, S.A. Blum, *ACS Catal.* 4 (2014) 622–629;  
 (c) J.J. Hirner, K.E. Roth, Y. Shi, S.A. Blum, *Organometallics* 31 (2012) 6843–6850.
- [6] W. Clegg, *Acta Crystallogr. Sect. B: Struct. Crystallogr. Cryst. Chem.* 34 (1978) 278–281.
- [7] B. Findeis, M. Contel, L.H. Gade, M. Laguna, I.J. Gimeno, M. McPartlin, *Inorg. Chem.* 36 (1997) 2386–2390.
- [8] D.M.P. Mingos, H.R. Powell, T.L. Stolberg, *Transit. Met. Chem.* 17 (1992) 334–337.
- [9] D. Joosten, I. Weissinger, M. Kirchmann, C. Maichle Mossmer, F.M. Schappacher, R. Pottgen, L. Wesemann, *Organometallics* 26 (2007) 5696–5701.
- [10] S. Hagen, I. Pantenburg, F. Weigend, C. Wickleder, L. Wesemann, *Angew. Chem. Int. Ed.* 42 (2003) 1501–1505.
- [11] R.D. Adams, V. Rassolov, Y.O. Wong, *Angew. Chem. Int. Ed.* 53 (2014) 11006–11009.
- [12] R.D. Adams, V. Rassolov, Q. Zhang, *Organometallics* 32 (2013) 6368–6378.
- [13] D.V. Partyka, M. Zeller, A.D. Hunter, T.G. Gray, *Angew. Chem. Int. Ed.* 45 (2006) 8188–8191.
- [14] SAINT+, Version 6.2a, Bruker Analytical X-ray Systems, Inc., Madison, WI, 2001.
- [15] G.M. Sheldrick, SHELXTL, Version 6.1, Bruker Analytical X-ray Systems, Inc., Madison, WI, 1997.
- [16] ADF2013; SCM Theoretical Chemistry, Vrije Universiteit, Amsterdam, The Netherlands, <http://www.scm.com>.
- [17] J.P. Perdew, A. Ruzsinszky, G.I. Csonka, O.A. Vydrov, G.E. Scuseria, *Phys. Rev. Lett.* 100 (2008) 136406.
- [18] D.M.P. Mingos, *Pure Appl. Chem.* 52 (1980) 705–712.
- [19] H.G. Raubenheimer, H. Schmidbaur, *Organometallics* 31 (2012) 2507–2522.
- [20] D.S. Weinberger, M. Melaimi, C.F. Moore, A.L. Rheingold, G. Frenking, P. Jerabek, G. Bertrand, *Angew. Chem. Int. Ed.* 52 (2013) 8964–8967.
- [21] A.A. Mohamed, A.P. Mayer, H.E. Abdou, M.D. Irwin, L.M. Perez, J.P. Fackler Jr., *Inorg. Chem.* 46 (2007) 11165–11172.
- [22] (a) C.M. Alvarez, M.A. Alvarez, M.E. Garcia, A. Ramos, M.A. Ruiz, M. Lanfranchi, A. Tiripicchio, *Organometallics* 24 (2005) 7–9;  
 (b) M.A. Alvarez, M.E. Garcia, A. Ramos, M.A. Ruiz, *Organometallics* 25 (2006) 5374–5380.
- [23] M.A. Alvarez, M.E. Garcia, D. Garcia-Vivo, M.A. Ruiz, M.F. Vega, *Organometallics* 29 (2010) 512–515.
- [24] A. Ugrinov, S.C. Sevol, *Chem. Eur. J.* 10 (2004) 3727–3733.
- [25] D.K. Srivastava, N.P. Rath, L. Barton, *Organometallics* 11 (1992) 2263–2273.
- [26] A. Bauer, A. Schier, H. Schmidbaur, *J. Chem. Soc. Dalton Trans.* (1995) 2919–2920.